



Photovoltaic Polymers Based on Difluoroquinoxaline Units With Deep HOMO Levels

Suhee Song,^{1,2} Sangha Keum,³ Ji-Hyun Lee,³ Jihoon Lee,¹ Seungmin Kim,¹
Seong Soo Park,³ Jin Young Kim,² Sung Heum Park,¹ Youngeup Jin ²

¹Department of Physics, Pukyong National University, Busan, 48513, Korea

²Department of Energy Engineering, Ulsan National Institute of Science and Technology (UNIST), Ulsan, 44919, South Korea

³Department of Industrial Chemistry, Pukyong National University, Busan, 48513, Korea

Correspondence to: Y. Jin (E-mail: yjin@pknu.ac.kr) or S. H. Park (E-mail: shpark@pknu.ac.kr)

Received 7 February 2018; accepted 26 March 2018; published online 00 Month 2018

DOI: 10.1002/pola.29014

ABSTRACT: We report the synthesis of low bandgap polymers with a difluoroquinoxaline unit by Stille polymerization for use in polymer solar cells (PSCs). A new series of copolymers with 2,3-didodecyl-6,7-difluoro quinoxaline as the electron-deficient unit and alkyloxybenzo[1,2-*b*:4,5-*b'*]dithiophene and thiophene as the electron-rich unit were synthesized. The photovoltaic properties of the devices based on the synthesized polymers revealed that the fluorine atoms at the quinoxaline units aid in decreasing the highest occupied molecular orbital (HOMO) energy levels; this in turn increased the open circuit voltage of the devices. The polymers with long alkyl chains exhibited good solubility that increased their molecular weight, but the

power conversion efficiency was low. Efficient polymer solar cells were fabricated by blending the synthesized copolymers with PC₇₁BM, and the PCE increased up to 5.11% under 100 mW cm⁻² AM 1.5 illumination. These results demonstrate that the importance of having a control polymer to be synthesized and characterized side by side with the fluorine analogues. © 2018 Wiley Periodicals, Inc. *J. Polym. Sci., Part A: Polym. Chem.* **2018**, *00*, 000–000

KEYWORDS: alkyl chain; fluorine atom; polymer; solar cells; synthesis

INTRODUCTION Organic photovoltaics (OPVs) have become a hot topic of research in the last two decades because of their high performance, reliance on potentially nontoxic and inexpensive materials, and ease of solution processing on lightweight and cost-effective flexible substrates.¹ Extensive research has been carried out to increase the power conversion efficiency (PCE) of OPVs by the synthesis of new materials,^{2–4} morphology control,^{2,5,6} and design of new device structure.^{2,7,8} A critical feature of polymer solar cells (PSCs), which are a class of OPVs, is the interface between an electron-donating polymer and an electron-accepting fullerene derivative.^{1,9} Bulk heterojunction (BHJ) structure have attracted significant interest, due to their potential advantages: (1) controlled HOMO energy levels, (2) ameliorated absorption spectrum, (3) improved mechanical/thermal properties, and (4) a high hole mobility from planar structure.¹⁰ The PCE of solar cell devices has been improved to over 10% by designing a new low-bandgap material and device optimization.^{11–14} In order to realize high photovoltaic performance, development of a low bandgap copolymer is very important to control the energy levels and optical

band gap of the donor material.¹⁵ Many low band gap conjugated polymers have been designed with electron deficient “acceptor (A)” type unit and electron rich “donor (D)” units to enhance the π - π stacking between polymer main chains, which was attributed intramolecular charge transfer (ICT) from electron donor to the electron acceptor.^{16,17}

Many of the low-bandgap conjugated polymers have an electron-withdrawing building block (e.g., benzothiadiazole (BT),^{18,19} 2*H*-benzimidazole,^{20,21} diketopyrrolopyrrole²² and 6,7-difluoroquinoxaline²³) and an electron-donating moiety (e.g., such as carbazole,²⁴ indenoindene,²⁵ cyclopentaphenanthrene,²⁰ and benzodithiophene.^{26–28} Benzodithiophene is a widely used electron donating materials because it readily undergoes polymerization and polymers of dialkoxy benzodithiophene provide high PCEs.²⁹ The quinoxaline moiety has been widely used as an electron acceptor in PSCs because the two N atoms at the 1,4-positions make the quinoxaline unit an electron-deficient molecule,^{30,31} and the two alkyl chains at its 2- and 3-positions lead to good solubility and tenability.³² Introduction of fluorine atom exhibits the effect on the energy

Additional Supporting Information may be found in the online version of this article.

© 2018 Wiley Periodicals, Inc.

of the charge transfer state caused by electron withdrawing effect of the fluorine atom. The hydrogen bond (C—H...F—C) reduces the distance between polymer chains, which induce improvement of charge transport and ordering.³³ The absorption of polymer with 6,7-difluoroquinoxaline was red-shifted compared to non-fluorinated analogue, attributed to the aggregated domain in solution.³⁴ Two fluorine atoms at the 6- and 7-positions of the quinoxaline moiety leads to lower highest occupied molecular orbital (HOMO) energy levels and good device performance.^{15,35} Conjugated polymers with deeper HOMO energy levels are conducive for achieving a higher open-circuit voltage (V_{oc}) and better PCE.³⁶ In addition, selection of a suitable alkyl chain to ensure good solubility is imperative because the alkyl chain influences the molecular weights, intermolecular interactions, morphology, and charge transport of the polymer.¹⁵ Moreover, high thermal stability of the polymers is crucial for preventing deformation of the polymer morphology, which is imperative for application in OPVs.

In this work, we designed and synthesized push-pull conjugated polymers based on 6,7-difluoroquinoxaline, benzodithiophene and different bridges such as thiophene (**P1** and **P2**), 3-hexylbithiophene (**P3**), and 4-hexylbithiophene (**P4**). To ensure good solubility, we introduced octyldodecyl chains in the benzodithiophene unit in **P1** and **P2**. The solubility of **P3** and **P4** greatly improved with the introduction of a hexyl chain at the bithiophene bridges. Conjugated polymers as promising candidate for high performance PSCs were synthesized by Stille polymerization. The thermal, optical, and electrochemical properties of the synthesized polymers were investigated. PSCs with the configuration ITO/PEDOT:PSS/polymer:PC₇₁BM/Al were fabricated for evaluating the photovoltaic properties of the polymers.

EXPERIMENTAL

Characterization

All reagents purchased from Aldrich or TCI were used without further purification. Solvents were purified by typical procedures and handled under moisture-free atmosphere. ¹H and ¹³C NMR spectra were recorded on a JNM ECP-400 (400 MHz, JEOL) spectrometer, and chemical shifts were recorded in ppm using TMS as the internal standard. Flash column chromatography was performed using Merck silica gel 60 (particle size 230–400 mesh ASTM) with a gradient elution of ethyl acetate/hexane or methanol/dichloromethane unless otherwise indicated. Analytical thin layer chromatography (TLC) was conducted using Merck 0.25-mm silica gel 60F pre-coated aluminum plates with a fluorescent indicator UV254. The molecular weight and polydispersity of the polymer were determined by gel permeation chromatography (GPC) with calibration using polystyrene standards. UV-vis absorption spectra were recorded on a Varian 5E UV-VIS-NIR spectrophotometer.

Synthesis of 5,8-dibromo-2,3-didodecyl-6,7-difluoroquinoxaline (**4**)

3,6-Dibromo-4,5-difluorobenzene-1,2-diamine (**3**) (2.2 g, 7.3 mmol) and 13,14-hexacosanedione (**2**) (3.48 g, 8.8 mmol) were dissolved in acetic acid (60 mL) and heated to 100

°C overnight. After the reaction mixture was cooled to room temperature, water and ethyl acetate were added. The aqueous phase was extracted with ethyl acetate and combined organic layer were dried over MgSO₄. The organic phase was concentrated under reduced pressure and the residue was purified by flash column chromatography to give 3.7 g of compound **4** as white solid. ¹H NMR (CDCl₃, 400MHz, δ): 3.03 (t, 4H, J = 7.66 Hz), 1.88 (m, 4H, J = 7.52 Hz), 1.24–1.44 (m, 36H), 0.86 (t, 6H, J = 6.84 Hz). ¹³C NMR (CDCl₃, 100MHz, δ): 158.17, 149.71 (d of d), 135.75, 109.23 (d of d), 34.62, 31.92, 29.68, 29.65, 29.58, 29.51, 29.45, 29.37, 29.31, 27.66, 22.69, 14.12. MS (m/z): calcd for C₃₂H₅₀Br₂F₂N₂, 658.2; found, 658.

Synthesis of 2,3-didodecyl-6,7-difluoro-5,8-di(2-thienyl)quinoxaline (**5**)

A solution of 5,8-dibromo-2,3-didodecyl-6,7-difluoroquinoxaline (**4**) (2.5 g, 3.8 mmol) and tributyl(2-thienyl)stannane (4.23 g, 11.4 mmol) in 60 mL of THF at room temperature was treated with dichlorobis(triphenylphosphine)palladium(II) (2 mol%). The reaction mixture was stirred for 12 h at 90 °C, concentrated under reduced pressure, and the residue was purified by flash column chromatography to give 2.1 g of compound **5** as a yellow solid. ¹H NMR (CDCl₃, 400MHz, δ): 7.98 (d, 2H, J = 2.96 Hz), 7.59 (d, 2H, J = 4.96 Hz), 7.21 (t, 2H, J = 4.56 Hz), 3.06 (t, 4H, J = 7.52 Hz), 1.96 (m, 4H, J = 7.45 Hz), 1.24–1.45 (m, 36H), 0.86 (t, 6H, J = 6.86 Hz). ¹³C NMR (CDCl₃, 100MHz, δ): 155.21, 148.82 (d of d), 134.53, 131.01, 130.41(d), 129.52, 126.33, 117.51, 34.68, 31.92, 29.72, 29.69, 29.66, 29.60, 29.57, 29.38, 29.37, 28.05, 22.69, 14.12. MS (m/z): calcd for C₄₀H₅₆Br₂N₂S₂, 666.4; found, 666.

Synthesis of 5,8-bis(5-bromo-2-thienyl)-2,3-didodecyl-6,7-difluoro quinoxaline (**6**)

2,3-Didodecyl-6,7-difluoro-5,8-di(2-thienyl) quinoxaline (**5**) (2.0 g, 3.0 mmol) was brominated with *N*-bromosuccinimide (NBS) (1.1 g, 6.0 mmol) in THF (60 mL) at room temperature. After stirring for 24 h, water (100 mL) and ethyl acetate (200 mL) were added. The aqueous phase was extracted with ethyl acetate and combined organic layer were dried over MgSO₄. The organic phase was concentrated under reduced pressure and the residue was purified by flash column chromatography to give 2.4 g of compound **6** as an orange solid. ¹H NMR (CDCl₃, 400MHz, δ): 7.75 (d, 2H, J = 4.00 Hz), 7.14 (d, 2H, J = 4.04 Hz), 3.08 (t, 4H, J = 7.66 Hz), 1.97 (m, 4H, J = 7.46 Hz), 1.23–1.46 (m, 36H), 0.85 (t, 6H, J = 6.84 Hz). ¹³C NMR (CDCl₃, 100MHz, δ): 155.42, 148.68 (d of d), 133.58, 132.60, 130.35, 129.03, 118.56, 116.61, 34.75, 31.93, 29.72, 29.70, 29.63, 29.59, 29.41, 29.38, 28.14, 22.70, 14.14. MS (m/z): calcd for C₄₀H₅₄Br₂F₂N₂S₂, 822.2; found, 822.

Synthesis of 2,3-didodecyl-6,7-difluoro-5,8-bis(3'-hexyl[2,2'-bithiophen]-5-yl)quinoxaline (**8**)

A solution of 5,8-bis(5-bromo-2-thienyl)-2,3-didodecyl-6,7-difluoro quinoxaline (**6**) (4.13 g, 5.0 mmol) and tributyl(3-hexylthiophen-2-yl)stannane (**7**) (6.88 g, 15.0 mmol) in 100 mL of DMF at room temperature was treated with

dichlorobis(triphenylphosphine)palladium(II) (2 mol%). The reaction mixture was stirred for 12 h at 90 °C, concentrated under reduced pressure, and the residue was purified by flash column chromatography to give 4.1 g of compound **8** as a yellow solid. ¹H NMR (CDCl₃, 400MHz, δ): 7.97 (d, 2H, J = 4.04 Hz), 7.21 (m, 4H, J = 4.00 Hz), 6.97 (d, 2H, J = 5.08Hz), 3.08 (t, 4H, J = 7.76 Hz), 2.86 (t, 4H, J = 7.80 Hz), 1.99 (m, 4H, J = 7.52 Hz), 1.68 (m, 4H, J = 7.49 Hz), 1.49-1.21 (m, 48H), 0.86 (m, 12H).

Synthesis of 5,8-bis(5'-bromo-3'-hexyl-[2,2'-bithiophen]-5-yl)-2,3-didodecyl-6,7-difluoroquinoxaline (**9**)

2,3-Didodecyl-6,7-difluoro-5,8-bis(3'-hexyl-[2,2'-bithiophen]-5-yl)quinoxaline (**8**) (4.1g, 4.1 mmol) as brominated with *N*-bromosuccinimide (NBS) (1.4 g, 8.1 mmol) in THF (12 mL) at room temperature. After stirring for 24 h, water (100 mL) and ethyl acetate (200 mL) were added. The aqueous phase was extracted with ethyl acetate and combined organic layer were dried over MgSO₄. The organic phase was concentrated under reduced pressure and the residue was purified by flash column chromatography to give 4.4 g of compound **9** as an orange solid. ¹H NMR (CDCl₃, 400MHz, δ): ¹H NMR (CDCl₃, 400MHz, δ): 7.95 (d, 2H, J = 3.76 Hz), 7.14 (d, 2H, J = 4.01Hz), 6.93 (d, 2H, J = 4.32 Hz), 3.07 (s, 4H), 2.78 (t, 4H, J = 2.68 Hz), 1.99 (s, 4H), 1.63 (s, 4H), 1.55-1.22 (m, 48H), 0.86 (m, 12H).

Synthesis of 2,3-didodecyl-6,7-difluoro-5,8-bis(4'-hexyl-[2,2'-bithiophen]-5-yl)quinoxaline (**11**)

A solution of 5,8-bis(5-bromo-2-thienyl)-2,3-didodecyl-6,7-difluoro quinoxaline (**6**) (4.1 g, 5.0 mmol) and tributyl(4-hexylthiophen-2-yl)stannane (**10**) (6.9 g, 15.0 mmol) in 100 mL of DMF at room temperature was treated with dichlorobis(triphenylphosphine)palladium(II) (2 mol%). The reaction mixture was stirred for 12 h at 90 °C, concentrated under reduced pressure, and the residue was purified by flash column chromatography to give 4.3 g of compound **11** as a yellow solid. ¹H NMR (CDCl₃, 400MHz, δ): 7.93 (d, 2H, J = 4.04 Hz), 7.22 (d, 2H, J = 4.01 Hz), 7.12 (d, 2H, J = 4.01 Hz), 6.84 (s, 2H) 3.10 (t, 4H, J = 7.24 Hz), 2.60 (t, 4H, J = 7.80 Hz), 2.06 (m, 4H), 1.54 (m, 4H), 1.50-1.17 (m, 48H), 0.86 (m, 12H).

Synthesis of 5,8-bis(5'-bromo-4'-hexyl-[2,2'-bithiophen]-5-yl)-2,3-didodecyl-6,7-difluoroquinoxaline (**12**)

2,3-Didodecyl-6,7-difluoro-5,8-bis(4'-hexyl-[2,2'-bithiophen]-5-yl) quinoxaline (**11**) (4.3 g, 4.3 mmol) was brominated with *N*-bromosuccinimide (NBS) (1.5 g, 8.5 mmol) in THF (60 mL) at room temperature. After stirring for 24 h, water (100 mL) and ethyl acetate (200 mL) were added. The aqueous phase was extracted with ethyl acetate and combined organic layer were dried over MgSO₄. The organic phase was concentrated under reduced pressure and the residue was purified by flash column chromatography to give 4.4 g of compound **12** as an orange solid. ¹H NMR (CDCl₃, 400MHz, δ): ¹H NMR (CDCl₃, 400MHz, δ): 7.90 (d, 2H, J = 3.76 Hz), 7.18 (d, 2H, J = 4.13Hz), 6.96 (s, 2H), 3.09 (t, 4H, J = 7.8Hz), 2.54 (t, 4H, J = 7.8 Hz), 2.06 (t, 4H, J = 7.00 Hz), 1.75 (t, 4H, J = 7.01 Hz), 1.54-1.21 (m, 48H), 0.86 (m, 12H).

Polymerization of poly[2,6-(4,8-bis(2-butyloctyloxy)benzo[1,2-*b*:4,5-*b'*]dithiophene)-alt-5,5'-(5,8-(bis-(2-thienyl))-6,7-difluoro-2,3-dihexylquinoxaline)] (**P1**)

Carefully purified 2,6-bis(trimethyltin)-4,8-bis(2-butyloctyloxy)benzo[1,2-*b*:4,5-*b'*]dithiophene (**13**) (0.62 g, 0.7 mmol), 5,8-bis(5-bromothiophen-2-yl)-6,7-difluoro-2,3-dihexylquinoxaline (**15**) (0.46 g, 0.7 mmol), P(*o*-tolyl)₃ (40 mol%), DMF (2 mL) and Pd₂(dba)₃ (3 mol%) were dissolved in 8 mL of chlorobenzene. The mixture was refluxed with vigorous stirring for 2 days under argon atmosphere. After cooling to room temperature, the mixture was poured into methanol. The precipitated material was recovered by filtration. The resulting solid material was reprecipitated using 100 mL of THF/1.0 L of methanol several times to remove residual amount of catalyst. The purified polymer was collected by filtration to give 577 mg as violet solid.

Polymerization of poly[2,6-(4,8-bis(2-butyloctyloxy)benzo[1,2-*b*:4,5-*b'*]dithiophene)-alt-5,5'-(5,8-(bis-(2-thienyl))-2,3-didodecyl-6,7-difluoroquinoxaline)] (**P2**)

By following the similar method used for **P1**, **P2** was synthesized with 2,6-bis(trimethyltin)-4,8-bis(2-butyloctyloxy)benzo[1,2-*b*:4,5-*b'*]dithiophene (**13**) (0.62 g, 0.7 mmol) and 5,8-bis(5-bromo-2-thienyl)-2,3-didodecyl-6,7-difluoroquinoxaline (**6**) (0.46 g, 0.7 mmol). The purified polymer was collected by filtration to give 490 mg as violet solid.

Polymerization of poly[2,6-(4,8-bis(2-ethylhexyloxy)benzo[1,2-*b*:4,5-*b'*]dithiophene)-alt-5,5'-(5,8-bis(3'-hexyl-[2,2'-bithiophen]-5-yl)-2,3-didodecyl-6,7-difluoroquinoxaline)] (**P3**)

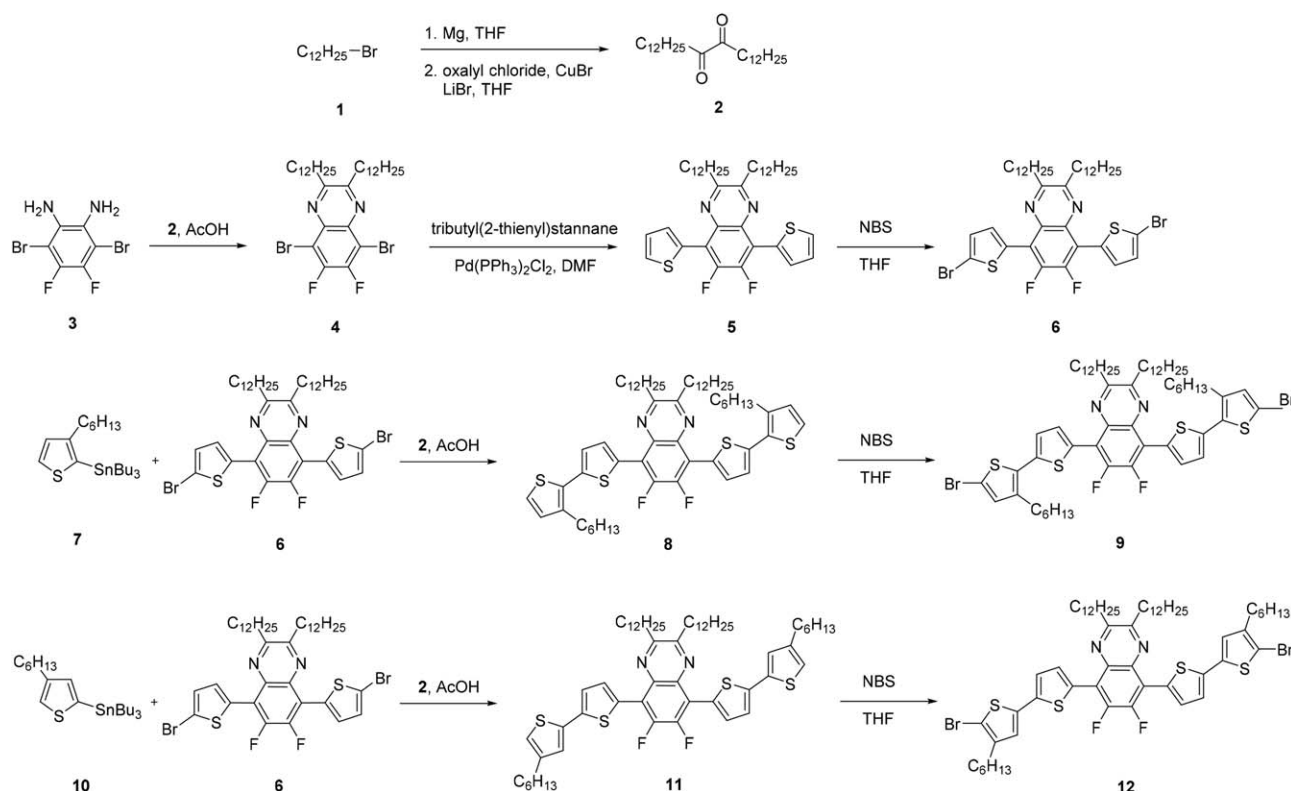
By following the similar method used for **P1**, **P3** was synthesized with (4,8-bis((2-ethylhexyl)oxy)benzo[1,2-*b*:4,5-*b'*]dithiophene-2,6-diyl)bis(trimethylstannane) (**14**) (0.39 g, 0.5 mmol) and 5,8-bis(5'-bromo-3'-hexyl-[2,2'-bithiophen]-5-yl)-2,3-didodecyl-6,7-difluoroquinoxaline (**9**) (0.58 g, 0.5 mmol). The purified polymer was collected by filtration to give 642 mg as violet solid.

Polymerization of poly[2,6-(4,8-bis(2-ethylhexyloxy)benzo[1,2-*b*:4,5-*b'*]dithiophene)-alt-5,5'-(5,8-bis(5'-bromo-4'-hexyl-[2,2'-bithiophen]-5-yl)-2,3-didodecyl-6,7-difluoroquinoxaline)] (**P4**)

By following the similar method used for **P1**, **P4** was synthesized with (4,8-bis((2-ethylhexyl)oxy)benzo[1,2-*b*:4,5-*b'*]dithiophene-2,6-diyl)bis(trimethylstannane) (**14**) (0.39 g, 0.5 mmol) and 5,8-bis(5'-bromo-4'-hexyl-[2,2'-bithiophen]-5-yl)-2,3-didodecyl-6,7-difluoroquinoxaline (**12**) (0.58 g, 0.5 mmol). The purified polymer was collected by filtration to give 554 mg as violet solid.

The Solar Cell Fabrication

Solar cells were fabricated on an indium tin oxide (ITO)-coated glass substrate with the following structure: ITO-coated glass substrate/poly(3,4-ethylenedioxythiophene):poly(stylenesulfonate) (PEDOT:PSS)/polymer:PCBM/Al. The ITO-coated glass substrate was first cleaned using a detergent and ultrasonicated in acetone and isopropyl alcohol, followed by drying overnight in an oven. PEDOT:PSS (Baytron PH) aqueous solution was spin-cast to form a 40 nm thick film. The substrate was dried for 10



SCHEME 1 Synthetic route of the monomers.

min at 140 °C in air and then transferred into a glove box to spin-cast the charge separation layer. A solution containing a mixture of polymer:PCBM in dichlorobenzene as solvent was then spin-casted on top of the PEDOT/PSS layer. Then, the film was dried for 60 min at 70 °C in the glove box. The sample was heated at 80 °C for 10 min in air. Then, an aluminum (Al, 100 nm) electrode was deposited by thermal evaporation under a vacuum of approximately 5×10^{-7} Torr. Current density-voltage (J - V) characteristics of the devices were measured using a Keithley 236 source measure unit. Solar cell performance was measured using an Air Mass 1.5 Global (AM 1.5 G) solar simulator with an irradiation intensity of 1000 W m^{-2} . An aperture (12.7 mm^2) was used on top of the cell to eliminate extrinsic effects such as cross-talk, and waveguiding, shadow effects. The spectral mismatch factor was calculated by the comparison of the solar simulator spectrum with the AM 1.5 spectrum at room temperature.

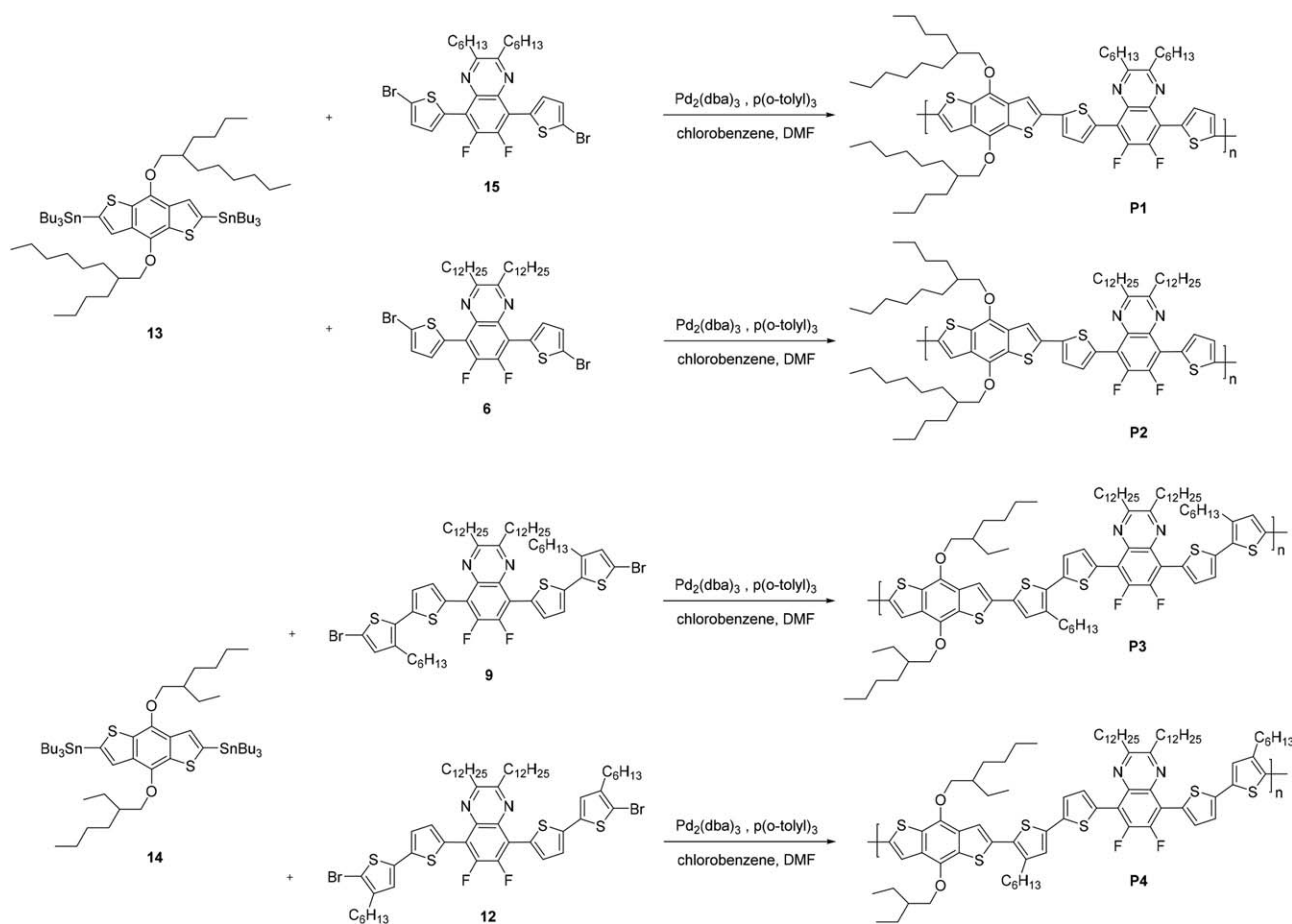
RESULTS AND DISCUSSION

Synthesis and Characterization

The synthetic routes to the monomers and polymers are outlined in Schemes 1 and 2, respectively. In the first step, 13,14-hexacosanedione (**2**) was prepared from oxalyl chloride via the Grignard reaction. 3,6-Dibromo-4,5-difluorobenzene-1,2-diamine (**3**) was coupled with compound **2** to obtain 5,8-dibromo-2,3-didodecyl-6,7-difluoroquinoxaline (**4**). Stille coupling of compound **4** with tributyl(2-thienyl)stannane afforded 2,3-didodecyl-6,7-difluoro-5,8-di(2-thienyl)-quinoxaline (**5**), which was brominated with

N-bromosuccinimide (NBS) to generate 5,8-bis(5-bromo-2-thienyl)-2,3-didodecyl-6,7-difluoro quinoxaline (**6**). Compound **6** was reacted with tributyl(3-hexylthiophen-2-yl)stannane (**7**) or tributyl(4-hexylthiophen-2-yl)stannane (**10**) through Stille coupling to obtain 2,3-didodecyl-6,7-difluoro-5,8-bis(3'-hexyl-[2,2'-bithiophen]-5-yl)quinoxaline (**8**) or 2,3-didodecyl-6,7-difluoro-5,8-bis(4'-hexyl-[2,2'-bithiophen]-5-yl)quinoxaline (**11**), respectively. Next, compound **8** or compound **11** were brominated with NBS in tetrahydrofuran (THF) to obtain 5,8-bis(5'-bromo-3'-hexyl-[2,2'-bithiophen]-5-yl)-2,3-didodecyl-6,7-difluoroquinoxaline (**9**) and 5,8-bis(5'-bromo-4'-hexyl-[2,2'-bithiophen]-5-yl)-2,3-didodecyl-6,7-difluoroquinoxaline (**12**), respectively. Copolymers with alkyloxybenzo[1,2-*b*:4,5-*b'*]dithiophene and thiophene as the electron-donating moiety and 2,3-dialkyl-6,7-difluoroquinoxaline as the electron-accepting unit were synthesized through Pd(0)-catalyzed Stille coupling polymerization in chlorobenzene. Two dodecyl chains in the quinoxaline moiety and a butyloctyloxy chain in the benzodithiophene moiety were introduced to improve the solubility of the polymers. All the synthesized polymers showed good solubility in organic solvents.

Table 1 summarizes the including molecular weight, polydispersity index (PDI) and thermal stability of the polymers. The molecular weights and PDIs of the polymers dissolved in chloroform were determined by gel permeation chromatography (GPC) using polystyrene as the standard. The number-average molecular weight (M_n) values for the polymers were 16,000–50,000 with PDI values of 1.2–2.4. **P2** has



SCHEME 2 Synthetic route of the polymers.

a higher molecular weight as compared with **P1** due to its better solubility resulting from longer alkyl chain at the quinoxaline units. Figure 1 shows the thermogravimetric analysis (TGA) curves, which indicate the thermal properties of the polymers. TGA was performed on a DuPont 951 TGA instrument under nitrogen, at a heating rate of 10 °C/min to 500 °C. The TGA curves revealed that the copolymers were thermally stable, with a weight loss of approximately 5% in the range 335–342 °C, in air.

Optical Properties

For the measurement of optical properties, a solution of each polymer in dichlorobenzene was prepared and spin-coated on

quartz plates to obtain a thin film. Figure 2 shows the UV-vis absorption spectra of the polymers in solution and thin film states. The maxima wavelength in solutions and in films, and absorption onsets are summarized in Table 1. **P1** and **P2** showed similar absorption spectra in solution, with the absorption maxima at 564 and 568 nm, respectively. The absorption spectra of **P3** and **P4** with alkylated thiophene units in solution showed absorption maxima at about 538 and 547 nm, respectively. The polymers with increasing numbers of thiophene rings show broad absorptions.³⁷ The absorption maxima of **P3** and **P4** in solution was blue-shifted as compared with those of **P1** and **P2** because of a larger average dihedral angle with longer donor segments,^{37,38} which

TABLE 1 Polymerization Results, Thermal and Optical properties of Polymers

Polymer	M_n^a (g/mol)	M_w^a (g/mol)	PDI ^a	TGA (T_d) ^b	in solution (nm)	in thin film (nm)
P1	38000	92000	2.4	336	564	574
P2	50000	120000	2.4	342	568	573
P3	21000	51000	2.4	335	538	564
P4	16000	19000	1.2	336	547	555

^a Molecular weight (M_w) and polydispersity (PDI) of the polymers were determined by gel permeation chromatography (GPC) in THF using polystyrene standards.

^b Onset decomposition temperature (5% weight loss) measured by TGA under N_2 .

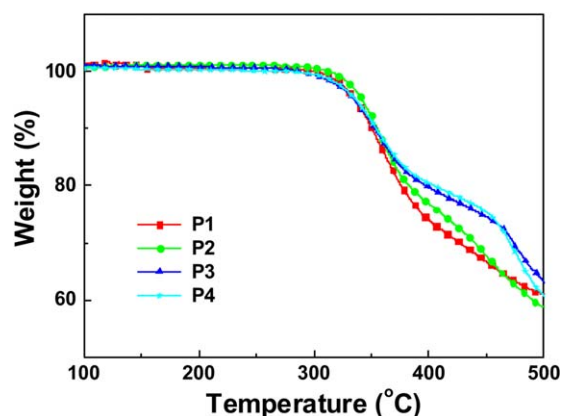


FIGURE 1 Thermogravimetric analysis of the polymers under N_2 . [Color figure can be viewed at wileyonlinelibrary.com]

can disrupt the planarity of the polymer backbone.³⁹ The absorption band of **P3** was blue-shifted as compared with that of **P4** caused by more larger dihedral angle of donor segment from 3-hexyl in thiophene.³⁷ The absorption band in the longer wavelength region (500–750 nm) could be assigned to the intramolecular charge transfer (ICT) transition from electron donor to the electron acceptor.³⁸ The peaks at ~ 600 nm of the polymer with bithiophene were weaker than those with

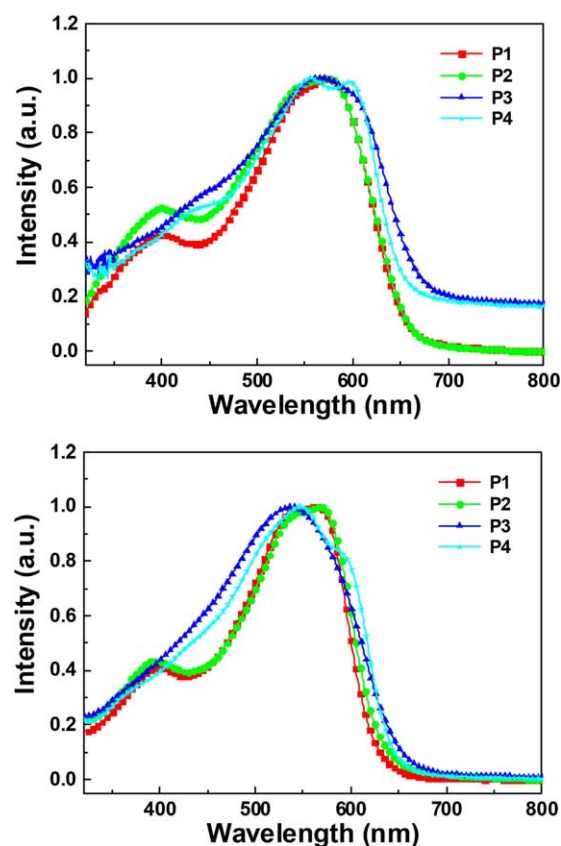


FIGURE 2 UV-visible absorption spectra of polymers in dichlorobenzene solution (a) and the solid state. [Color figure can be viewed at wileyonlinelibrary.com]

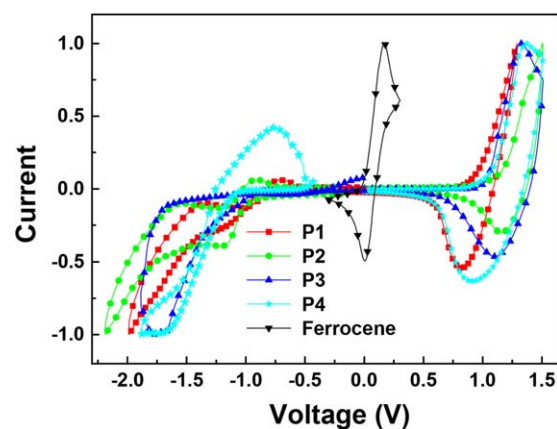


FIGURE 3 Electrochemical properties of polymers. [Color figure can be viewed at wileyonlinelibrary.com]

mono thiophene, illustrating that the electron-rich moiety weakens the intramolecular charge transfer (ICT) transitions.³⁹ The spectra of the synthesized polymers in solid films exhibited absorption bands with λ_{\max} at 555–574 nm and absorption onset at 652–671 nm, corresponding to band gaps of 1.85–1.90 eV. The absorption bands in films exhibited a significant red-shift and broader as compared to those in solution caused by interchain π -stacking.^{40,41}

Electrochemical and Theoretical Calculations

The electrochemical properties of the polymers were determined using the band gap estimated from the absorption onset and the HOMO energy level estimated by cyclic voltammetry (CV). CV was performed with a solution of tetrabutylammonium tetrafluoroborate (Bu_4NBF_4) (0.10 M) in acetonitrile at a scan rate of 100 mV/s at room temperature under argon. A platinum electrode (~ 0.05 cm²) coated with a thin polymer film was used as the working electrode; a Pt wire and Ag/AgNO₃ electrode were used as the counter and reference electrodes, respectively. The energy level of the Ag/AgNO₃ reference electrode (calibrated by the Fc/Fc⁺ redox system) was 4.8 eV below the vacuum level.

Figure 3 shows the CV spectra of the polymers, and Table 2 summarizes their oxidation potentials derived from the onsets of electrochemical p-doping. The HOMO and lowest unoccupied molecular orbital (LUMO) levels were calculated according to the empirical formula ($E_{HOMO} = -([E_{\text{onset}}]^{\text{ox}} + 4.8)$ eV) and ($E_{LUMO} = -([E_{\text{onset}}]^{\text{red}} + 4.8)$ eV), respectively. The oxidation potential onsets of the synthesized polymers ranged from 0.80 to 0.87 V, corresponding to the HOMO energy levels from -5.60 to -5.61 eV. Since the length of the substituted alkyl chain does not affect the HOMO energy levels, the synthesized polymers had similar HOMO energy levels. The reduction onset potentials ranged from -0.82 to -1.09 V vs. Ag/Ag⁺. The LUMO energy levels were calculated to be in the range -3.71 to -3.98 eV. Electrochemical band gaps, calculated from CV data, were determined to be 1.63–1.95 eV. The HOMO energy levels of the fluorinated polymers were lower because of the electron-withdrawing effect of the fluorine atoms, leading to higher V_{OC} values.^{42,43}

TABLE 2 Electrochemical Potentials and Energy Levels of the Polymers

Polymers	Optical band gap ^a (eV)	HOMO ^b (eV)	LUMO ^c (eV)	E_{ox}^{d} (V)	$E_{\text{red}}^{\text{d}}$ (V)	Electrochemical band gap ^e (eV)
P1	1.89	-5.61	-3.98	0.81	-0.82	1.63
P2	1.87	-5.60	-3.97	0.80	-0.83	1.63
P3	1.85	-5.60	-3.71	0.80	-1.09	1.89
P4	1.90	-5.67	-3.72	0.87	-1.08	1.95

^a Optical energy band gap was estimated from the onset wavelength of the optical absorption.

^b Calculated from the oxidation potentials.

^c Calculated from the reduction potentials.

^d Onset oxidation and reduction potential measured by cyclic voltammetry.

^e Calculated from the E_{ox} and E_{red} .

The optimized geometries were calculated at the B3 LYP/6-31G (d,p) level of theory using the Gaussian 03 package.⁴⁴ The HOMO and LUMO surfaces were plotted using the GaussView version 4.1. For simplicity, the alkyl chains were replaced with methyl groups and only one repeating unit, **M1**, **M3**, or **M4**, was used for the simulation of **P1** (or **P2**), **P3**, or **P4**, respectively. The optimized structures of **M1**, **M3** and **M4** are shown in Figure 4. The HOMO wave functions of the repeating units are usually delocalized along the entire polymer backbone, while the LUMO wave function is localized onto the electron-

rich unit (6,7-difluoroquinoxaline unit). The introduction of bithiophene into the polymer decreased the electron density at the difluoroquinoxaline moiety due to the weak push-pull effect. Due to the enhanced conjugation length by the inserted alkyl-thiophene with respect to the monomer of polymer, the HOMO energy level was raised by about 0.31 eV. The repeating unit (**WO**) that had bithiophene without the alkyl chain led to decreased electron density at the quinoxaline unit, which was confirmed to exhibit no effect on the alkyl chain at bithiophene.

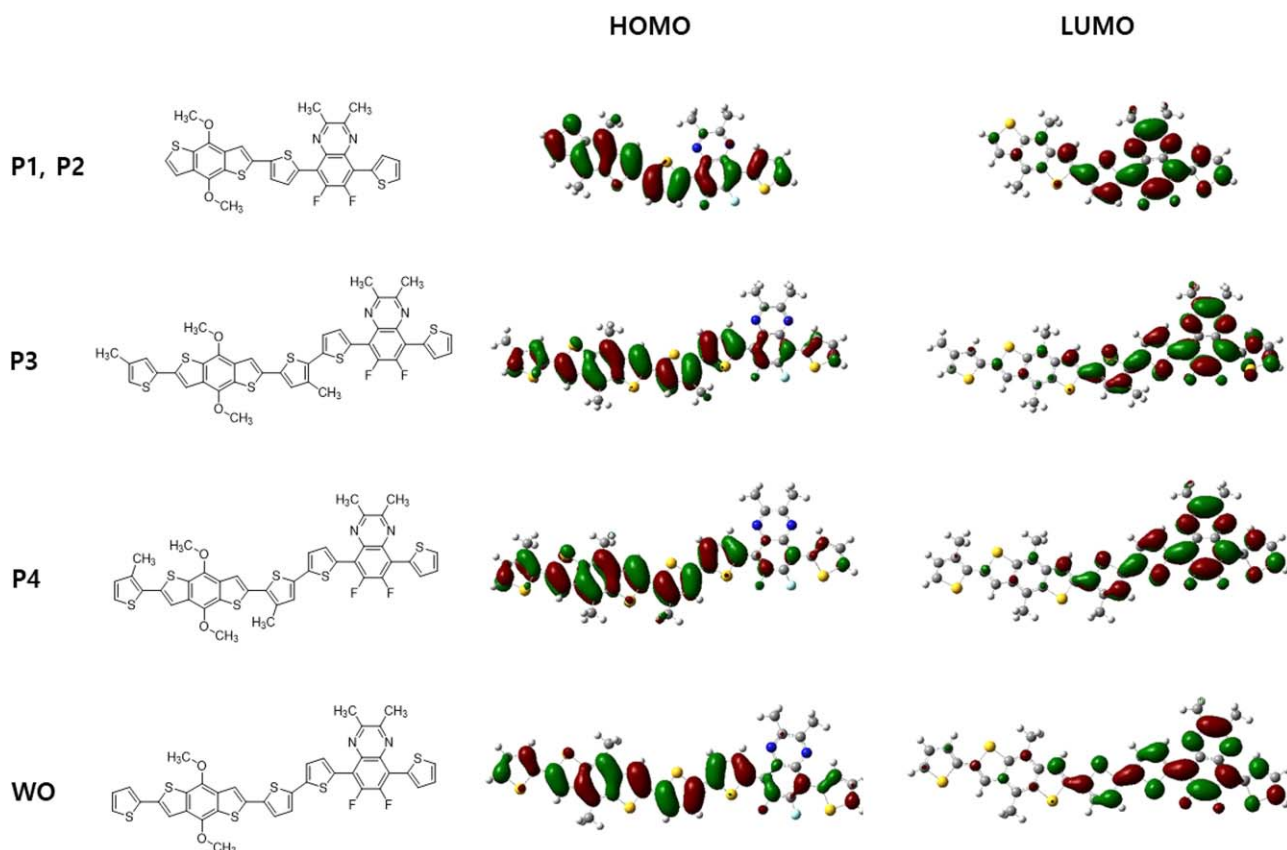


FIGURE 4 Theoretical calculation of the monomers by density functional theory (DFT) at the B3LYP/6-31G level. [Color figure can be viewed at wileyonlinelibrary.com]

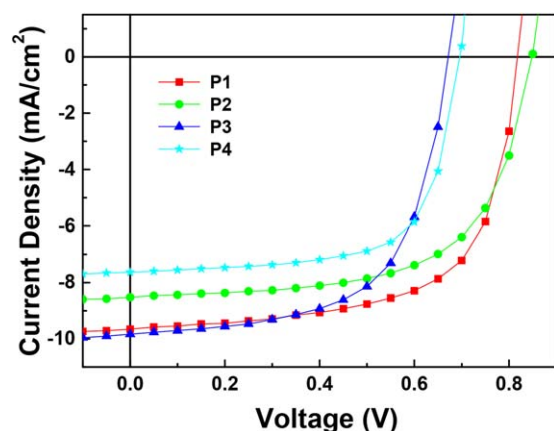


FIGURE 5 Current density-potential characteristics of the polymer solar cells under the illumination of AM 1.5, 100 mW/cm². [Color figure can be viewed at wileyonlinelibrary.com]

Photovoltaic Properties of Synthesized Polymers

Photovoltaic cells based on the synthesized polymers were fabricated by spin coating a dichlorobenzene solution of the PC₇₁BM polymers. Figure 5 summarizes the photovoltaic properties measured for the devices with the following configuration, ITO/PEDOT:PSS (40 nm)/polymer:PC₇₁BM (80 nm)/Al (100 nm), under AM 1.5G irradiation (100 mW/cm²), and Table 3 summarizes the values obtained. The device comprising **P1**:PCBM at a concentration of 1.5 wt% in dichlorobenzene exhibited a V_{OC} of 0.82, short-circuit current density (J_{SC}) of 9.66 mA/cm², and fill factor (FF) of 0.65, respectively corresponding to a PCE of 5.11%. The corresponding values for the device with **P2**:PCBM were 0.85 V, 8.52 mA/cm², and 0.63, affording a PCE of 4.54%. The device based on **P3** and **P4** with bithiophene units showed V_{OC} of 0.67 and 0.70 V, J_{SC} of 9.83 and 7.63 mA/cm², and FF of 0.62 and 0.68, giving a PCE of 4.07% and 3.61%, respectively. Although the polymers with bithiophene units show a large conjugated area, **P3** and **P4** exhibit localization electron density at benzothiophene unit to decrease PCE.

The incident-photon-to-current efficiency (IPCE) spectra of the photovoltaic devices from the polymer:PCBM blends are presented in Figure 6. The spectra showed maxima of 71.5% at 410 nm for **P1**, 55.9% at 430 nm for **P2**, 71.1% at 390 nm for **P3** and 53.8% at 390 nm for **P4**. The enhanced efficiency of **P1** was due to the higher IPCE between 300 and 800 nm. The surface morphologies of the photovoltaic films were determined through atomic force microscopy (AFM) measurements in Supporting Information. AFM images (surface area of $2 \times 2 \mu\text{m}^2$

TABLE 3 Photovoltaic Properties of the Polymer Solar Cells

Polymers	J_{SC} (mA/cm ²)	V_{OC} (V)	FF	PCE (%)
P1	9.66	0.82	0.65	5.11
P2	8.52	0.85	0.63	4.54
P3	9.83	0.67	0.62	4.07
P4	7.63	0.70	0.68	3.61

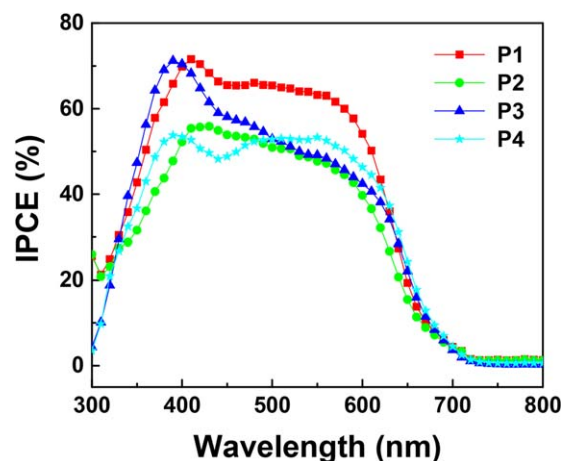


FIGURE 6 IPCE curves of the corresponding polymer solar cells. [Color figure can be viewed at wileyonlinelibrary.com]

by the tapping mode) obtained from the polymer:PC₇₁BM blend films. Although the blend films of **P1** and **P2** showed similar morphological properties (aggregation sizes and features), the more homogeneous surface of **P1** led to a higher PCE.

CONCLUSIONS

We used Stille coupling polymerization to prepare new conjugated polymers with benzo[1,2-*b*:4,5-*b'*]dithiophene moieties and 2,3-dialkyl-6,7-difluoroquinoxaline units in the main backbone. The HOMO energy levels of the synthesized polymers were -5.60 to -5.61 eV, which demonstrated that the electron-withdrawing effect of the fluorine atoms decreased the HOMO levels. The device comprising **P1**:PCBM at a concentration of 1.5 wt% in dichlorobenzene exhibited a V_{OC} of 0.82 V, J_{SC} of 9.66 mA/cm², and FF of 0.65, affording a PCE of 5.11%. This series of synthesized polymers with 2,3-dialkyl-6,7-difluoroquinoxaline units possess a large potential for higher performance PSCs.)

ACKNOWLEDGMENT

This work was supported by a Research Grant of Pukyong National University (2017–2018).

REFERENCES

- 1 K. R. Graham, C. Cabanetos, J. P. Jahnke, M. N. Idso, A. Labban, G. O. N. Ndjawa, T. Heumueller, K. Vandewal, A. Salleo, B. F. Chmelka, A. Amassian, P. M. Beaujuge, M. D. McGehee, *J. Am. Chem. Soc.* **2014**, *136*, 9608.
- 2 J. Zhang, Y. Zhang, J. Fang, K. Lu, Z. Wang, W. Ma, Z. Wei, *J. Am. Chem. Soc.* **2015**, *137*, 8176.
- 3 Y. J. Cheng, S. H. Yang, C. S. Hsu, *Chem. Rev.* **2009**, *109*, 5868.
- 4 P. L. T. Boudreault, A. Najari, M. Leclerc, *Chem. Mater.* **2010**, *23*, 456.

- 5 G. Li, V. Shrotriya, J. S. Huang, Y. Yao, T. Moriarty, K. Emery, Y. Yang, *Nat. Mater.* **2005**, *4*, 864.
- 6 J. Peet, J. Y. Kim, N. E. Coates, W. L. Ma, D. Moses, A. J. Heeger, G. C. Bazan, *Nat. Mater.* **2007**, *6*, 497.
- 7 J. Y. Kim, K. Lee, N. E. Coates, D. Moses, T. Q. Nguyen, M. Dante, A. J. Heeger, *Science* **2007**, *317*, 222.
- 8 Z. He, C. Zhong, X. Huang, W.-Y. Wong, H. Wu, L. Chen, S. Su, Y. Cao, *Adv. Mater.* **2011**, *23*, 4636.
- 9 D. Beljonne, J. Cornil, L. Muccioli, C. Zannoni, J.-L. Brédas, F. Castet, *Chem. Mater.* **2011**, *23*, 591.
- 10 C. Lee, H. Kang, W. Lee, T. Kim, K. H. Kim, H. Y. Woo, C. Wang, B. J. Kim, *Adv. Mater.* **2015**, *27*, 2466.
- 11 W. Zhao, S. Li, H. Yao, S. Zhang, Y. Zhang, B. Yang, J. Hou, *J. Am. Chem. Soc.* **2017**, *139*, 7148.
- 12 Y. Liu, J. Zhao, Z. Li, C. Mu, W. Ma, H. Hu, K. Jiang, H. Lin, H. Ade, H. Yan, *Nat. Commun.* **2014**, *5*, 5293.
- 13 H. J. Cho, Y. J. Kim, S. Chen, J. Lee, T. J. Shin, C. E. Park, C. Yang, *Nano Energy* **2017**, *39*, 229.
- 14 J. Lee, D. H. Sin, B. Moon, J. Shin, H. G. Kim, M. Kim, K. Cho, *Energy Environ. Sci.* **2017**, *10*, 247.
- 15 H. Hu, K. Jiang, G. Yang, J. Liu, Z. Li, H. Lin, Y. Liu, J. Zhao, J. Zhang, F. Huang, Y. Qu, W. Ma, H. Yan, *J. Am. Chem. Soc.* **2015**, *137*, 14149.
- 16 K. Li, Z. Li, K. Feng, X. Xu, L. Wang, Q. Peng, *J. Am. Chem. Soc.* **2013**, *135*, 13549.
- 17 Z. Zeng, Y. Li, J. Deng, Q. Huang, Q. Peng, *J. Mater. Chem. A* **2014**, *2*, 653.
- 18 S. H. Park, A. Roy, S. Beaupre, S. Cho, N. Coates, J. S. Moon, D. Moses, M. Leclerc, K. Lee, A. J. Heeger, *Nat. Photonics* **2009**, *3*, 297.
- 19 N. Blouin, A. Michaud, M. Leclerc, *Adv. Mater.* **2007**, *19*, 2295.
- 20 S. Song, Y. Jin, S. H. Park, S. Cho, I. Kim, K. Lee, A. J. Heeger, H. Suh, *J. Mater. Chem.* **2010**, *20*, 6517.
- 21 S. Song, J. Kim, J. Shim, J. Kim, B. H. Lee, Y. Jin, I. Kim, K. Lee, H. Suh, *Sol. Energ. Mat. Sol. C* **2012**, *98*, 323.
- 22 I. Welterlich, O. Charov, B. Tieke, *Macromolecules* **2012**, *45*, 4511.
- 23 S. Song, H. I. Choi, I. S. Shin, H. Suh, M. H. Hyun, G. D. Lee, S. S. Park, S. H. Park, Y. Jin, *Bull. Korean Chem. Soc.* **2014**, *35*, 2245.
- 24 S. Song, S. H. Park, Y. Jin, I. Kim, K. Lee, H. Suh, *Polymer* **2010**, *51*, 5385.
- 25 S. Song, Y. Jin, S. H. Kim, J. Moon, K. Kim, J. Y. Kim, S. H. Park, K. Lee, H. Suh, *Macromolecules* **2008**, *41*, 7296.
- 26 H. H. Cho, T. E. Kang, K. H. Kim, H. Kang, H. J. Kim, B. J. Kim, *Macromolecules* **2012**, *45*, 6415.
- 27 L. Dou, J. Gao, E. Richard, J. You, C. C. Chen, K. C. Cha, Y. He, G. Li, Y. Yang, *J. Am. Chem. Soc.* **2012**, *134*, 10071.
- 28 Y. Liang, D. Feng, Y. Wu, S. T. Tsai, G. Li, C. Ray, L. Yu, *J. Am. Chem. Soc.* **2009**, *131*, 7792.
- 29 Q. V. Hoang, C. E. Song, S. J. Moon, S. K. Lee, J. C. Lee, B. J. Kim, W. S. Shin, *Macromolecules* **2015**, *48*, 3918.
- 30 K. W. Song, T. H. Lee, E. J. Ko, K. H. Back, D. K. Moon, *J. Polym. Sci. Pol. Chem.* **2014**, *52*, 1028.
- 31 M. Liu, Y. Gao, Y. Zhang, Z. Liub, L. Zhaoa, *Polym. Chem.* **2017**, *8*, 4613.
- 32 S. Song, T. Kim, D. Kang, H. Suh, M. H. Hyun, S. S. Park, G. D. Lee, J. Y. Kim, Y. Jin, *Polym. Bull.* **2016**, *73*, 2511.
- 33 R. Kroon, R. Gehlhaar, T. T. Steckler, P. Henriksson, C. Muller, J. Bergqvist, A. Hadipour, P. Heremans, M. R. Andersson, *Sol. Energ. Mat. Sol. C* **2012**, *105*, 280.
- 34 A. Iyer, J. Bjorgaard, T. Anderson, M. E. Köse, *Macromolecules* **2012**, *45*, 6380.
- 35 Y. Q. Zheng, Z. Wang, J. H. Dou, S. D. Zhang, X. Y. Luo, Z. F. Yao, J. Y. Wang, J. Pei, *Macromolecules* **2015**, *48*, 5570.
- 36 D. Liu, W. Zhao, S. Zhang, L. Ye, Z. Zheng, Y. Cui, Y. Chen, J. Hou, *Macromolecules* **2015**, *48*, 5172.
- 37 Q. Tao, Y. Xia, X. Xu, S. Hedström, O. Bäcke, D. I. James, P. Persson, E. Olsson, O. Inganäs, L. Hou, W. Zhu, E. Wang, *Macromolecules* **2015**, *48*, 1009.
- 38 J. H. Kim, J. B. Park, H. U. Kim, I. N. Kang, D. H. Hwang, *Synth. Met.* **2014**, *194*, 88.
- 39 K. Lu, J. Fang, H. Yan, X. Zhu, Y. Yi, Z. Wei, *Organic Electronics* **2013**, *14*, 2652.
- 40 Q. Fan, H. Jiang, Y. Liu, W. Su, H. Tan, Y. Wang, R. Yang, W. Zhu, *J. Mater. Chem. C* **2016**, *4*, 2606.
- 41 S. Wen, C. Wang, P. Ma, Y. X. Zhao, C. Li, S. Ruan, *J. Mater. Chem. A* **2015**, *3*, 13794.
- 42 H. Bronstein, J. M. Frost, A. Hadipour, Y. Kim, C. B. Nielsen, R. S. Ashraf, B. P. Rand, S. Watkins, I. McCulloch, *Chem. Mater.* **2013**, *25*, 277.
- 43 S. Tang, P. Murto, X. Xu, C. Larsen, E. Wang, L. Edman, *Chem. Mater.* **2017**, *29*, 7750.
- 44 M. J. Frisch, G. W. Trucks, H. B. Chlengel, G. E. Scuseria, M. A. Robb, J. R. Cheeseman, J. A. Montgomery Jr., T. Vreven, K. N. Kudin, J. C. Burant, J. M. Millam, S. S. Iyengar, J. Tomasi, V. Barone, B. Mennucci, M. Cossi, G. Scalmani, N. Rega, G. A. Petersson, H. Nakatsuji, M. Hada, M. Ehara, K. Toyota, R. Fukuda, J. Hasegawa, M. Ishida, T. Nakajima, Y. Honda, O. Kitao, H. Nakai, M. Klene, X. Li, J. E. Knox, H. P. Hratchian, J. B. Cross, V. Bakken, C. Adamo, J. Jaramillo, R. Gomperts, R. E. Stratmann, O. Yazyev, A. J. Austin, R. Cammi, C. Pomelli, J. W. Ochterski, P. Y. Ayala, K. Morokuma, G. A. Voth, P. Salvador, J. J. Dannenberg, V. G. Zakrzewski, S. Dapprich, A. D. Daniels, M. C. Strain, O. Farkas, D. K. Malick, A. D. Rabuck, K. Raghavachari, J. B. Foresman, J. V. Ortiz, Q. Cui, A. G. Baboul, S. Clifford, J. Cioslowski, B. B. Stefanov, G. Liu, A. Liashenko, P. Piskorz, I. Komaromi, R. L. Martin, D. J. Fox, T. Keith, M. A. Al-Laham, C. Y. Peng, A. Nanayakkara, M. Challacombe, P. M. W. Gill, B. Johnson, W. Chen, M. W. Wong, C. Gonzalez, J. A. Pople, Gaussian 03, Revision E.01, Gaussian Inc., Wallingford, CT, USA, **2004**.